Silicon surface passivation by transparent conductive zinc oxide

Journal of Applied Physics

Silicon surface passivation by transparent conductive zinc oxide

Cite as: J. Appl. Phys. **125**, 105305 (2019); https://doi.org/10.1063/1.5054166
Submitted: 30 August 2018 . Accepted: 31 January 2019 . Published Online: 14 March 2019

B. W. H. van de Loo, B. Macco, J. Melskens, W. Beyer, and W. M. M. Kessels

Journal of Applied Physics ARTICLE scitation.org/journal/jap

Silicon surface passivation by transparent conductive zinc oxide

Cite as: J. Appl. Phys. **125**, 105305 (2019); doi: 10.1063/1.5054166
Submitted: 30 August 2018 · Accepted: 31 January 2019 ·
Published Online: 14 March 2019

B. W. H. van de Loo,[1,2,a)] B. Macco,[1] J. Melskens,[1] W. Beyer,[3] and W. M. M. Kessels[1]

AFFILIATIONS

[1]Department of Applied Physics, Eindhoven University of Technology, P.O. Box 513, 5600 MB Eindhoven, The Netherlands
[2]Tempress Systems, 8171 MD Vaassen, The Netherlands
[3]IEK-5, Forschungszentrum Jülich GmbH, 52425 Jülich, Germany

[a)]bvdloo@tempress.nl

ABSTRACT

Surface passivation is essential for high-efficiency crystalline silicon (c-Si) solar cells. Despite the common use of transparent conductive oxides (TCOs) in the field of solar cells, obtaining surface passivation by TCOs has thus far proven to be particularly challenging. In this work, we demonstrate outstanding passivation of c-Si surfaces by highly transparent conductive ZnO films prepared by atomic layer deposition. Effective surface recombination velocities as low as 4.8 cm/s and 11 cm/s are obtained on 3 Ω cm *n*- and *p*-type (100) c-Si, respectively. The high levels of surface passivation are achieved by a novel approach by using (i) an ultrathin SiO_2 interface layer between ZnO and c-Si, (ii) a sacrificial Al_2O_3 capping layer on top of the ZnO film during forming gas annealing, and (iii) the extrinsic doping of the ZnO film by Al, B, or H. A combination of isotope labeling, secondary-ion mass spectrometry, and thermal effusion measurements showed that the sacrificial Al_2O_3 capping layer prevents the effusion of hydrogen from the crystalline ZnO and the underlying Si/SiO_2 interface during annealing, which is critical in achieving surface passivation. After annealing, the Al_2O_3 capping layer can be removed from the ZnO film without impairing the high levels of surface passivation. The surface passivation levels increase with increased doping levels in ZnO, which can be attributed to *field-effect* passivation by a reduction in the surface hole concentration. The ZnO films of this work are suitable as a transparent conductor, an anti-reflection coating, and a surface passivation layer, which makes them particularly promising for simplifications in future solar cell manufacturing.

I. INTRODUCTION

The passivation of electronic defect states at the crystalline silicon (c-Si) surface has been a topic of research already for decades, due to its large impact on the performance of silicon-based devices. For c-Si solar cells specifically, surface defect states induce the Shockley-Read-Hall recombination of light-generated charge carriers,[1,2] a process in which their free energy is lost for further power conversion. Therefore, in high-efficiency solar cells, the Si surface is typically being passivated by a thin film. Such surface passivation generally relies on the reduction of the interface defect density, referred to as *chemical* passivation, and the reduction of either the electron or hole concentration at the surface, referred to as *field-effect* passivation. While to date numerous materials are being used for surface passivation in c-Si solar cells, they are typically either electrically insulating (e.g., Al_2O_3, SiN_x, and SiO_2), or not transparent to the solar spectrum [e.g., hydrogenated amorphous silicon (a-Si:H) and polycrystalline silicon (poly-Si)], which restricts their applicability in solar cells. A highly transparent and conductive passivation layer would be ideal for the application at the front surface of solar cells, as it can, besides providing passivation, also assist in the current collection. Although in the last few years several new passivation materials have been discovered,[3] including AlN,[4] TiO_x,[5] GaO_x,[6] TaO_x,[7] HfO_x,[8] PO_x,[9] NbO_x,[10] and ZrO_x,[11] sufficient passivation by a transparent conductive oxide (TCO) has not yet been achieved. In this work, we report on outstanding passivation of the c-Si surface by ZnO, a material that is widely used in the field of photovoltaics as TCO.

ZnO is an abundant n-type semiconductor with a wide and direct optical bandgap ($E_g > 3.2$ eV), making it transparent for most of the solar spectrum. The refractive index of $n \sim 2$ at 2 eV makes the ZnO films of 60–80 nm in thickness well-suited as an anti-reflection coating for c-Si solar cells. The carrier density and hence the work function of ZnO can accurately be controlled by the incorporation of extrinsic n-type dopants in the ZnO films, such as Al, B, Ga, or H.[12–16] Due to the above-mentioned properties and the relatively low work function of ~4.4 eV, ZnO is customarily being used as a transparent window layer to collect the current from (non-transparent) carrier-selective contact materials, such as doped c-Si, a-Si:H, or poly-Si.[17] Interestingly, TCOs could also in principle be used as a carrier-selective contact with Si. Already in the late 1960s, TCOs had been explored as electron-selective contact materials in rudimentary Si solar cells.[18] Also, ZnO specifically has recently been explored as electron-selective material for c-Si solar cells[19–21] or as an integral part of a hole-selective tunneling contact.[22] Most notably, Ding *et al.* have recently achieved a solar cell efficiency of 17% using the ZnO films as electron-selective contact for lowly-doped c-Si.[21] Nevertheless, it was found that the insertion of an intrinsic a-Si:H layer between the c-Si and the ZnO strongly improved the open-circuit voltage of the solar cell from 645 to 672 mV,[21] as the a-Si:H layer substantially improved the level of surface passivation.

From the above, it is clear that the transparent ZnO films thus potentially can be used as an electrical conductor, anti-reflection coating, passivation layer, and carrier-selective contact in c-Si solar cells. Yet, achieving surface passivation by TCOs, including ZnO, has thus far proven to be particularly challenging. Only recently, passivation by highly doped ZnO was demonstrated with an implied open-circuit voltage iV_{oc} of 650 mV by Panigrahi *et al.*[23] Such a level of passivation may, however, be insufficient for most high-efficiency c-Si solar cells. Note also that other transparent materials that are currently of high interest as, e.g., electron- or hole-selective contact, such as MoO_x,[24] WO_x,[25] and V_2O_5,[25] are commonly being restricted by a lack of surface passivation and are therefore typically used in combination with passivating a-Si:H interlayers. Understanding how Si surface passivation can be reached therefore remains a highly relevant research question.

In attempting to find a new route to enable excellent surface passivation by ZnO (which is a polycrystalline material), it is instructive to look at poly-Si passivating contacts that are well-known for their ability to provide excellent passivation to c-Si surfaces. In poly-Si passivating contacts, highly n- or p-type doped poly-Si layers are typically prepared on top of an ultra-thin SiO_2 interfacial oxide layer of 1-2 nm thickness (commonly termed "tunnel oxide"). The preparation method of this interfacial oxide layer is key in achieving high levels of surface passivation.[26] Additionally, after preparation, the SiO_2/poly-Si stack is typically being hydrogenated to further enhance the surface passivation levels. Such hydrogenation can be realized by exposing the poly-SI films to a remote hydrogen plasma,[27] or alternatively, by capping the poly-Si by thin films of Al_2O_3 or SiN_x followed by thermal annealing.[28–31]

In this work, we adopted a similar approach as the poly-Si case to investigate surface passivation by highly transparent and conductive ZnO films. Specifically, we explore the use of an ultra-thin interface oxide and an Al_2O_3 capping layer to achieve surface passivation by highly-doped ZnO films that are prepared by atomic layer deposition (ALD). In this way, we show that the ZnO films can provide excellent passivation to both n- and p-type c-Si surfaces. In addition, we scrutinize the passivation mechanisms using a combination of isotope labeling, secondary-ion mass spectrometry (SIMS), and thermal effusion measurements. Finally, the influence of the ZnO doping level on the passivation is demonstrated.

II. EXPERIMENTAL DETAILS

As substrates for lifetime measurements, 280-μm thick n- and p-type polished floatzone c-Si (100) wafers with a base resistivity of 3 Ω cm were used. Before the deposition of ZnO, the wafers received various pre-treatments, which were either:

(i) Radio Corporation of America (RCA) standard cleans 1 and 2[32] (which leave a thin SiO_2 layer at the c-Si surface),
(ii) the RCA cleans followed by a dip in diluted hydrofluoric acid (HF, 1%),
(iii) the RCA cleans, an HF dip and a subsequent nitric acid oxidation step (NAOS) for 15 min at room temperature.

After these various surface treatments, the lifetime samples were exposed to an inductively-coupled plasma with oxygen (4 s at a plasma power of 200 W). This plasma treatment was required to initiate the ALD of ZnO on surfaces which received the NAOS treatment. Immediately afterwards, the doped ZnO films were prepared by ALD. More specifically, Al-doped ZnO (ZnO:Al), B-doped ZnO (ZnO:B), or hydrogen-doped ZnO (ZnO:H) films were prepared on both sides of the lifetime samples in an Oxford Instruments OpAL™ reactor at 200 °C. The thickness of the ZnO films was ~75 nm, unless stated otherwise. The deposition of ZnO was carried out using diethylzinc (DEZ) and H_2O as precursors. Aluminum dopants were incorporated in the ZnO:Al films by using "supercycles" with dopant cycle ratio $m = 15$, meaning that every 15 ALD cycles of ZnO were followed by 1 ALD cycle of "Al_2O_3" using trimethylaluminum (TMA) and H_2O.[12] The ZnO:B films were prepared in a similar way with varying m, using triisopropyl borate (TIB) and H_2O as precursors during the dopant cycle.[13] Hydrogen was incorporated in the ZnO:H films by remote plasma treatments.[16] Note that the highly doped ZnO films already have been prepared in high-throughput *spatial* ALD reactors that are designed for high volume manufacturing in photovoltaic industries.[15] As a reference to the ALD ZnO films, 70 nm ZnO:Al films were also prepared by sputter deposition in a Kurt J. Lesker reactor at 155 °C, using ZnO:Al targets with 2 wt. % Al, and a plasma power density of 0.56 W/cm^2. For selected samples, the ZnO films

were capped by 30 nm of Al_2O_3, prepared by ALD at 200 °C using TMA and H_2O as precursors. Post-deposition annealing was carried out in a step-wise fashion at various temperatures (250, 300, 350, 400, 450 °C) in either forming gas (FGA) or nitrogen ambient in a Jipelec rapid thermal anneal furnace.

The thickness and optical properties of the films were determined by spectroscopic ellipsometry (SE). The SE data of the ZnO films were modelled using Tauc-Lorentz and Drude oscillators, following the approach of Knoops *et al.*[33] Hall measurements were carried out in the van der Pauw configuration to derive the resistivity ρ, the electron density N_e, and electron mobility μ_e of the as-deposited ZnO films on wafers with a thick thermal SiO_2 layer. The effective minority carrier lifetime τ and the iV_{oc} were determined by generalized photoconductance decay measurements using a Sinton Instruments WCT120. Thermal effusion measurements were carried out by heating samples at a constant rate of 20 °C/min in a quartz tube. The effused species were detected by a quadrupole-mass spectrometer. SIMS measurements were carried out at Philips Innovation Services.

III. RESULTS AND DISCUSSION

A. Surface passivation by ALD ZnO

Figure 1 shows the effective minority carrier lifetime for various lifetime samples passivated by 70 nm ALD ZnO:B. In the as-deposited state, ZnO:B did not provide any surface passivation to *n*-type Si, as is evident from the very low effective lifetime values (sample 1). Moreover, the effective lifetime

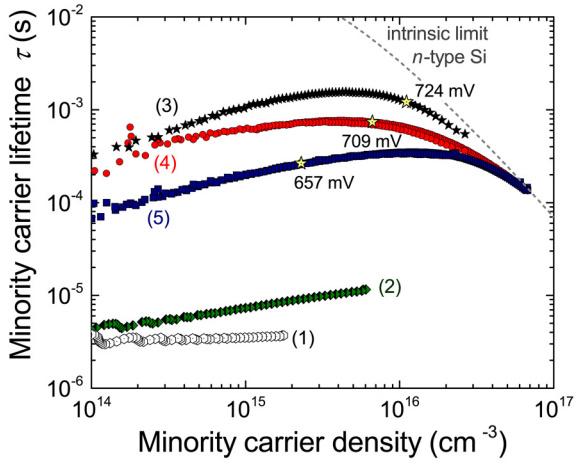

FIG. 1. Effective minority carrier lifetime of *n*-type c-Si samples passivated by ALD ZnO:B. Sample (1) received RCA cleans and was subsequently capped by ~75 nm ZnO:B. Sample (2) is as (1) but after FGA at 450 °C for 30 min. For sample (3), the ZnO:B was capped by ALD Al_2O_3 prior to FGA. Sample (4) is based on *p*-type Si which received the RCA 1 and 2 cleans, ZnO:B, Al_2O_3 capping, and FGA. Sample (5) is as (3), with additional HF dip after RCA cleans and FGA up to 475 °C. Stars indicate the implied open-circuit voltage under 1-sun illumination. The upper limit of the lifetime is calculated using the parameterization of the intrinsic recombination by Richter *et al.*[34]

improved only marginally by a subsequent 30-min FGA at 450 °C (sample 2). However, in the case that the as-deposited ZnO:B films were capped by Al_2O_3 films, excellent passivation could be achieved after such FGA, with $\tau = 1.53$ ms (at $\Delta n = 5 \cdot 10^{15}$ cm^{-3}) for *n*-type Si and $iV_{oc} = 724$ mV (sample 3). This lifetime corresponds to effective surface recombination velocities as low as $S_{eff} = 4.8$ cm/s when accounting for the intrinsic recombination parameterization of Richter *et al.*[34] The same conditions resulted also for *p*-type Si in outstanding levels of surface passivation, with $iV_{oc} = 709$ mV, $\tau = 760\,\mu$s, and $S_{eff} = 11$ cm/s (sample 4).

It was found that an appropriate surface treatment prior to the deposition of ZnO was essential to achieve the high levels of surface passivation. For example, for *n*-type Si wafers which received an HF dip prior to the ZnO deposition, a significantly lower level of surface passivation was obtained, with $\tau = 312\,\mu$s and $iV_{oc} = 657$ mV (sample 5). The dopant type in ZnO is, however, found to be of minor influence on the achievable passivation levels. For instance, using Al rather than B as *n*-type dopant, a similar level of surface passivation was reached for identical dopant levels, with $\tau = 1.58$ ms and $iV_{oc} = 725$ mV (not shown). Furthermore, the thickness of the ZnO film was not critical in achieving surface passivation either (see, e.g., Fig. S1 in the supplementary material). For example, a passivation test with 13 nm instead of 75 nm thick ZnO:Al films (both having the same doping level) resulted in a similar high lifetime value of $\tau = 1.2$ ms.

Figure 2 shows a high-resolution cross-sectional transmission electron microscopy (TEM) image of the passivating stack. It can be observed that the ZnO:B film is ~73 nm thick and polycrystalline and forms a sharp interface with a uniform SiO_2 interface oxide of 1.5 ± 0.1 nm in thickness. On top of the ZnO:B, part of the amorphous ALD Al_2O_3 capping layer is visible. The optical and electrical properties corresponding to the ZnO:B film of Fig. 2 are summarized in Table I. To evaluate the case that the ~73 nm thick ZnO:B passivation layer serves as an anti-reflection coating on random-pyramid textured silicon, the maximum short-circuit current density $J_{sc,max}$ of a solar cell under AM1.5G illumination was simulated by OPAL2.[35] In this simulation, no encapsulation (e.g., by EVA or glass) or any rear contacting materials were taken into account. The optical properties of the ZnO:B film derived from SE measurements were used as input for the simulation (see Table S1 in the supplementary material). The resulting J_{sc} of 41.6 mA/cm^2 for ZnO is comparable to J_{sc} values obtained when simulating optimized SiN_x layers as anti-reflection coating in OPAl2 ($J_{sc} = 42.9$ mA/cm^2). This underlines that the conductive and passivating ZnO:B films of this work are also very suitable as an anti-reflection coating for c-Si solar cells

B. Influence of interface pretreatments, annealing conditions, and deposition method on the surface passivation

In Sec. III A, it was found that the passivation quality provided by ZnO relies on the (chemical) pretreatment of the

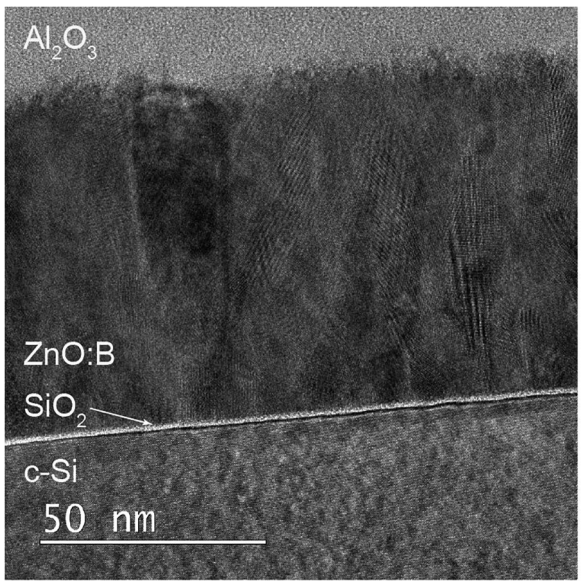

FIG. 2. High-resolution transmission electron microscopy image of a c-Si (100) wafer, passivated by ~73 nm ZnO:B. The c-Si wafer received the RCA 1 and 2 cleans prior to ZnO:B deposition. On top of the ZnO:B film, an Al_2O_3 capping film is present. The sample has received a 30-min forming gas anneal at 450 °C.

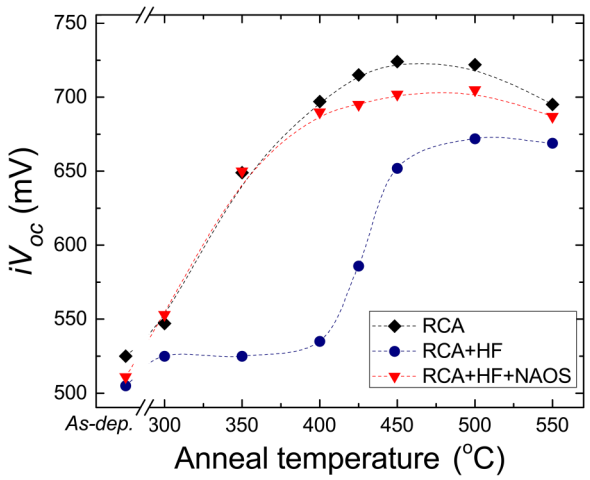

FIG. 3. The implied open-circuit voltage under 1-sun illumination for *n*-type c-Si lifetime samples passivated by 50 nm ZnO:Al and 30 nm Al_2O_3. Data are shown for cumulative annealing steps of 5 min in forming gas. The wafers received prior to ALD either (i) the RCA standard cleans 1 and 2, (ii) the RCA cleans followed by a dip in 1% HF, or (iii) the RCA, HF, and NAOS treatments.

c-Si surface. To investigate the influence of pretreatments in more detail, in Fig. 3, the passivation quality provided by 50-nm ZnO:Al is compared for different surface pretreatments as a function of the annealing temperature.

As can be seen, the highest iV_{oc} was achieved for the RCA-cleaned samples after annealing up to 450 °C. Most likely, at higher annealing temperatures, hydrogen effuses from the film stacks and the passivation worsens. For the samples that received an HF-dip after the RCA cleans, lower overall passivation levels were obtained. Moreover, the passivation in this case only increases from ~425 °C onwards. This can potentially be attributed that at these temperatures, a (better) interface oxide is formed. In case a surface oxide layer was re-grown after the HF–dip by a NAOS treatment (which leaves a 1.1-1.3 nm thick interface oxide[26]), a high iV_{oc} was again reached, comparable to the RCA-treated samples, with $\tau = 1.02$ ms. Apparently, the presence of a high-quality interface oxide is helpful for achieving high levels of surface passivation by ZnO:Al, as has been found for several other passivating materials as well.[26,36,37] Also, interface oxide layers grown by UV-ozone oxidation showed good surface passivation with ZnO, with lifetime values >1.5 ms.

Note that also other materials than SiO_2 may be used as interface oxide to achieve surface passivation. For instance, an ultra-thin layer of TiO_2—a material which is currently of high interest for Si solar cells due to its passivating contact properties[38]—also resulted in excellent surface passivation. Specifically, a 2.5-nm thick TiO_2 layer prepared by thermal ALD on an HF-dipped c-Si wafer capped by ZnO:Al and AlO_3 showed a similar trend with annealing as the samples with the NAOS and RCA treated surfaces, reaching $iV_{oc} = 689$ mV and $\tau = 755$ us. Note that this is one of the few examples in the literature where surface passivation is reached when TiO_2 is combined with a TCO.

When using interface oxides with a thickness in the ~nm range, it is important that the tunnel oxide is not damaged during the subsequent deposition of ZnO in order to achieve surface passivation. To illustrate this, besides ALD also sputter deposition was explored as a preparation method for ZnO:Al films. In analogy to previous experiments, the sputtered ZnO:Al films were capped by 30-nm thick ALD Al_2O_3 films and subjected to FGA in a stepwise fashion. Despite the same experimental procedure (except the ZnO deposition), only very low effective minority carrier lifetimes of ~30 μs were achieved for RCA-treated lifetime samples with sputtered ZnO:Al films. The large differences in surface

TABLE I. Summary of physical properties corresponding to the ALD ZnO:B film of Fig. 2. The iV_{oc} was obtained on *n*-type c-Si after capping the ZnO:B films by Al_2O_3 and a subsequent FGA up to 450 °C.

Physical property	Value
Thickness	73 nm
Resistivity	9.87×10^{-4} Ω cm
Carrier density	4.05×10^{20} cm^{-3}
Electron mobility	15.6 cm^2/V s
Tauc optical bandgap	3.73 eV
Refractive index (at 2.0 eV)	1.84
$J_{sc,max}$ (simulated by OPAL2)	41.6 mA/cm^2
Implied open-circuit voltage	725 mV

passivation quality between samples with ALD and sputtered ZnO films can be explained by the "soft deposition" nature of ALD compared to sputtering. For instance, it has been reported by Macco *et al.* that the sputter deposition of TCOs on thin a-Si:H passivation layers results in the significant reduction of the passivation quality due to plasma damage by ion-bombardment or UV-photons, whereas no reduction in passivation quality was observed when the ZnO was deposited by ALD.[14] Note that the TEM cross-section in Fig. 2 shows that the ALD ZnO layer forms a sharp interface with the underlying SiO_2 interface oxide, which could be indicative of such "soft" deposition. It is plausible that surface passivation can be achieved by sputtered ZnO films when such plasma damage can be mitigated.

C. The influence of the ALD Al_2O_3 capping layer on the interface hydrogenation

The lifetime results of Fig. 1 already showed that poor levels of surface passivation were obtained when the ZnO films were not capped by Al_2O_3 prior to annealing. In fact, when the ZnO films without Al_2O_3 capping layer were annealed in forming a gas at 450 °C, stains appeared on ZnO, which originate from mild etching of ZnO by hydrogen during the FGA. Such stains did not appear on similar samples that were annealed in nitrogen ambient. Nevertheless, also after prolonged annealing in nitrogen ambient, no surface passivation could be achieved by the ZnO films without Al_2O_3 capping layer. The presence of the Al_2O_3 capping layer is thus apparently critical in achieving surface passivation.

To understand how the Al_2O_3 capping layer assists in achieving surface passivation by the ZnO films, secondary ion-mass spectrometry and thermal effusion measurements were carried out on samples with and without Al_2O_3 capping layer. The results are shown in Figs. 4–6. To facilitate the tracing of the hydrogen throughout the passivation stack, for selected experiments the Al_2O_3 was prepared using deuterated TMA [i.e., $Al(CD_3)_3$] and D_2O as precursors rather than $Al(CH_3)_3$ and H_2O.

Figure 4 shows the distribution of hydrogen throughout ZnO:B films and ZnO:B/Al_2O_3 passivation stacks as obtained

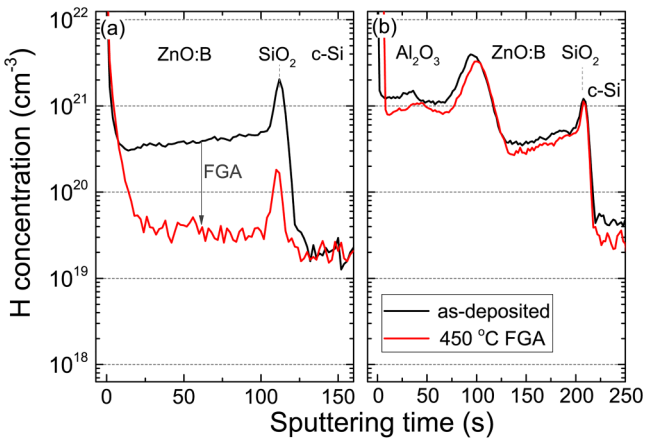

FIG. 4. Hydrogen depth profiles determined from SIMS of (a) ZnO:B and (b) ZnO:B/Al_2O_3 film stacks on c-Si with RCA oxide, before and after forming gas anneal for 30 min at 450 °C.

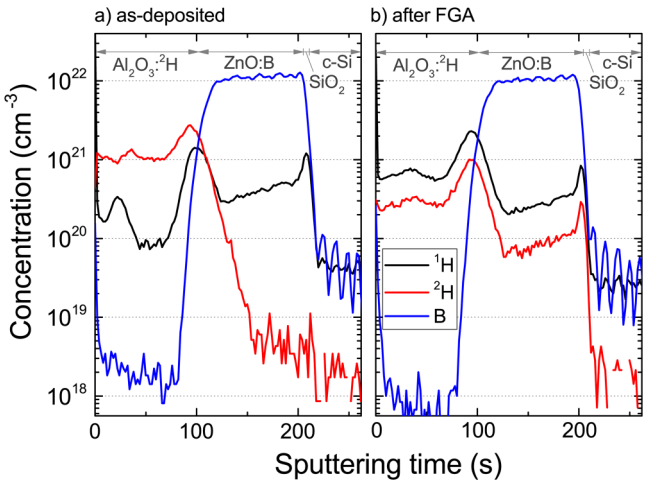

FIG. 5. Depth profiles of hydrogen, deuterium and boron measured by SIMS for Al_2O_3:^{2}H/ZnO:B stacks on c-Si with an RCA oxide in (a) the as-deposited state and (b) after FGA at 450 °C for 30 min. The relative uncertainty for [^{1}H] in ZnO is ±30% and for [^{2}H] is ~200%. Note that the [B] signal was not calibrated.

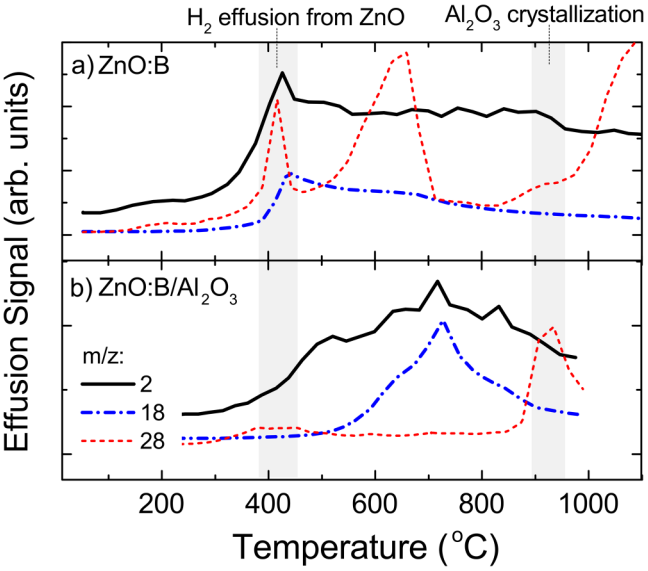

FIG. 6. Thermal effusion spectra of (a) ZnO:B films and (b) ZnO:B/Al_2O_3 stacks on c-Si. The temperature increases steadily at 20 °C /min. The *m/z* values correspond predominantly to the effusion of H_2 (*m/z* = 2), H_2O (*m/z* = 18), and CO (*m/z* = 28).

with SIMS. Without Al_2O_3 capping layer, a relatively high concentration of hydrogen was present in as-deposited ZnO:B and at the underlying SiO_2 interface layer [Fig. 4(a)]. However, the amount of hydrogen in the ZnO:B film as well as in the SiO_2 film is reduced by over an order of magnitude after FGA. In contrast, for the samples that were capped by Al_2O_3, the amount of hydrogen in the ZnO and the underlying SiO_2 interlayer remained high after FGA, and similar in concentration to as-deposited samples. Importantly, the hydrogen concentration at the c-Si/SiO_2 interface remains high after annealing in presence with the Al_2O_3 capping layer. The differences in hydrogen concentration at the c-Si/SiO_2 interface between the annealed capped and uncapped ZnO samples could well explain the observed differences in surface passivation quality.

The large difference in hydrogen concentration between the capped and uncapped ZnO samples after annealing can qualitatively be well-explained by the results in Figs. 5 and 6. When considering the isotope labeling results of Fig. 5, a complete redistribution of ^1H and ^2H throughout the entire passivation stack is observed after annealing, which demonstrates that hydrogen became very mobile during the FGA at 450 °C. Specifically, in the as-deposited state, a high concentration of ^2H was present in the Al_2O_3:^2H, whereas the ZnO:B film contained predominantly hydrogen. After FGA however, ^2H and ^1H followed a similar distribution profile throughout the entire film stack. Note that a large part of the deuterium in the SiO_2/ZnO/Al_2O_3 system has exchanged with hydrogen from the forming gas during annealing, as has also been observed in comparable isotope labeling experiments on SiO_2/poly-Si/Al_2O_3 stacks.[31]

Thermal effusion measurements in Fig. 6 reveal a strong effusion of H_2 around 400 °C for the uncapped ZnO films, whereas such effusion was not observed for samples that were capped by Al_2O_3. The rapid redistribution of deuterium in ZnO and the effusion of H_2 during annealing at ~400 °C have also been observed by Beyer *et al.*, who attributed this to the fast transport of molecular hydrogen through interconnected voids, i.e., the ZnO grain boundaries.[39] As the amorphous Al_2O_3 capping layer prepared at 200 °C does not allow for the transport of molecular hydrogen at 400–450 °C,[40] it is plausible that the capping layer impedes the transport and consecutive effusion of molecular hydrogen through the grain boundaries of ZnO and the underlying SiO_2 interlayer. This would explain why the hydrogen concentration of ZnO films that are capped with Al_2O_3 remains high after annealing. Note that in addition to blocking the effusion of molecular hydrogen from ZnO, the Al_2O_3 capping layer might also act as a hydrogen source for the underlying films during annealing. This is also supported by Fig. 5, which shows high concentrations of ^2H—originating from the Al_2O_3:^2H—at the passivated c-Si/SiO_2 interface after FGA.

Altogether, the variety of experimental results demonstrates that sufficient hydrogen should remain present at the c-Si/SiO_2 interface after annealing to passivate Si dangling bonds. For samples which were not annealed, the lack of sufficient surface passivation can be explained as, apart from having sufficient hydrogen at the c-Si/SiO_2 interface, also the thermal budget provided by the FGA is needed to activate chemical passivation of Si dangling bonds, as has, e.g., also been found for SiO_2/poly-Si/Al_2O_3 passivation stacks.[31] The Al_2O_3 helps in achieving surface passivation by ZnO as it suppresses a rapid effusion of hydrogen from the ZnO and the underlying c-Si/SiO_2 interface during FGA. After such FGA, we have verified that the Al_2O_3 capping layer can be removed from the passivation stack by highly diluted HF without severely impairing the surface passivation (with corresponding lifetimes of 1.31 and 1.08 ms prior to and after the removal of the Al_2O_3 layer, respectively). Therefore, the Al_2O_3 capping layer thus also can be used as a *sacrificial* layer which only needs to be present during annealing. Note that HF etches both Al_2O_3 as well as ZnO. Therefore, a carefully timed etch is required to minimalize the etching of the ZnO layer. However, in principle, ALD Al_2O_3 can be etched with high selectivity (>400:1) over ALD ZnO.[41]

The beneficial effect of a sacrificial Al_2O_3 capping layer on the (chemical) surface passivation has also been reported for other materials, including SiO_2[40,42,43] and SiO_2/poly-Si.[30] For the case of SiO_2/poly-Si, other dense capping layers can also be used for interface hydrogenation, such as SiN_x.[30] Potentially, such other dense and amorphous materials could therefore serve as capping material to enable passivation by ZnO as well.

D. Influence of the ZnO doping level on the field-effect passivation

It is well known that surface recombination can be reduced by reducing either the electron or the hole concentration at the surface. Such "field-effect passivation" can be induced by, e.g., a fixed charge density or the work function of a passivation layer. For ZnO, the work function can be effectively lowered by the addition of extrinsic *n*-type dopants.[12] Figure 7 shows the effect of the electron density for extrinsically doped ZnO films on the effective minority carrier lifetime.

Interestingly, the lifetime increases strongly with the electron density in ZnO. This can most likely be related to a change in field-effect passivation. Specifically, the evaluation of the Tauc optical bandgap of the ZnO films shows an increase from 3.25 eV for the lowest electron density ($N_e = 8.0{\cdot}10^{19}\,cm^{-3}$) to 3.73 eV for the film with the highest electron density (i.e., $N_e = 4.05{\cdot}10^{20}\,cm^{-3}$). This strong increase in the optical bandgap by ~0.5 eV is known as the Burstein-Moss shift[44,45] and can be primarily attributed to the shift of the Fermi level into the conduction band of ZnO, and thus a lowered work function.[12] Simulations of the c-Si/SiO_2/ZnO band alignment in Fig. 8 show how such a change in the doping level and work function affect the field-effect passivation. In this example, the hole concentration at the c-Si surface is three orders of magnitude lower in the case of highly-doped ZnO than for lowly-doped ZnO. The highly-doped ZnO yields a surface hole concentration which is eight orders of magnitude lower than the electron concentration at the surface. This asymmetry in carrier concentrations at the

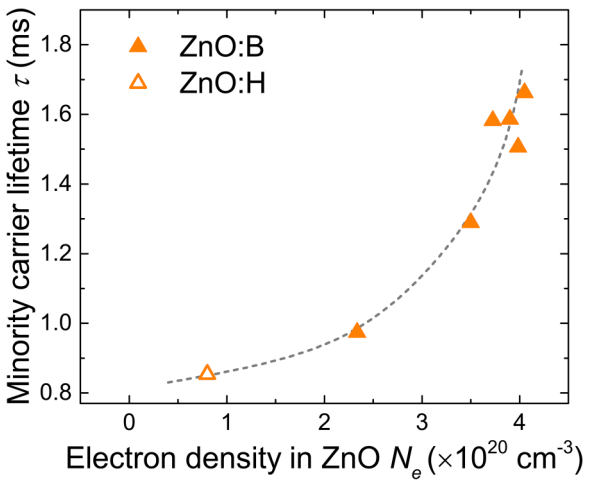

FIG. 7. Effective minority carrier lifetime at an injection level of $\Delta n = 5 \cdot 10^{15}\,\mathrm{cm}^{-3}$ for 3 Ω cm, RCA-treated *n*-type c-Si, passivated by ZnO/Al_2O_3 stacks after FGA at 450 °C for 30 min. Boron- and hydrogen-doped ZnO films with varying doping levels were used. The dashed line serves as a guide to the eye.

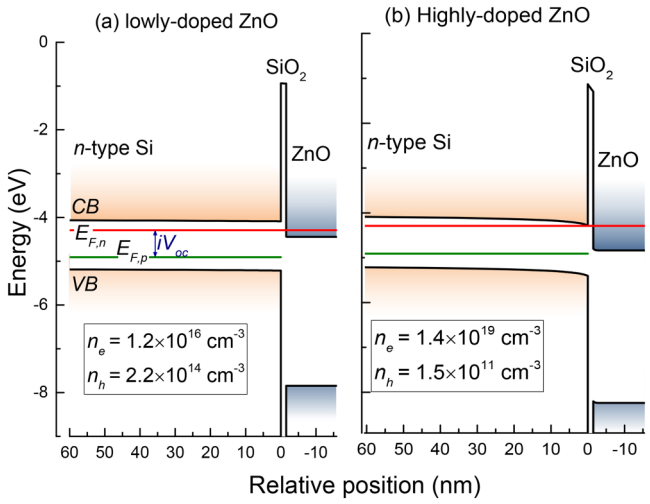

FIG. 8. The energy band alignment of c-Si/SiO_2/ZnO stacks as obtained from solving the Poisson equation using Fermi-Dirac statistics in COMSOL Multiphysics for (a) lowly doped ZnO with $N_e = 1.0 \times 10^{20}\,\mathrm{cm}^{-3}$ and (b) highly doped ZnO with $N_e = 6.5 \times 10^{20}\,\mathrm{cm}^{-3}$. The *x*-axis denotes the distance to the c-Si surface. The electron and hole concentrations at the c-Si surface are indicated. As input for the simulations, 3 Ω cm *n*-type Si with a base injection level $\Delta n = 10^{15}\,\mathrm{cm}^{-3}$ and an electron affinity of 4.05 eV were taken. The electron affinity of ZnO was set at 4.4 eV. The thickness of the SiO_2 interlayer was 1.5 nm, whereas the fixed charge density of the SiO_2 was assumed to be slightly positive, i.e., $Q_f = 5 \times 10^{11}\,\mathrm{cm}^{-2}$. The conduction band *CB*, valence band *VB*, and the quasi-Fermi levels for electrons E_{Fn} and holes E_{Fp} are indicated.

surface can significantly reduce the recombination rate through surface defect states, as this will be limited by the capturing of holes. Note that the ZnO films evaluated in this work have electron densities up to $\sim 4 \cdot 10^{20}\,\mathrm{cm}^{-3}$, while in principle electron densities of $\sim 10^{21}\,\mathrm{cm}^{-3}$ can even be reached for highly-doped ZnO.[46] This thus leaves the potential for further enhancements of the field-effect passivation.

IV. CONCLUSION AND OUTLOOK

We have demonstrated that the ALD ZnO films can provide excellent passivation of lowly-doped *n*- and *p*-type c-Si surfaces. It was found that the presence of a high-quality SiO_2 interface layer between c-Si and ZnO was key in achieving high levels of surface passivation. Moreover, it was required to cap ZnO by Al_2O_3 prior to FGA to obtain surface passivation. SIMS and thermal effusion measurements showed that the Al_2O_3 capping layer prevents the effusion of hydrogen from ZnO and the underlying c-Si/SiO_2 interface. Such effusion can most likely be attributed to the rapid transport of molecular hydrogen through the ZnO grain boundaries. After FGA, Al_2O_3 can be removed from ZnO without impairing the improved levels of passivation, making it possible to use Al_2O_3 as a "sacrificial" layer. Finally, it has been established that the level of surface passivation improves with increasing electron densities in the ZnO films. The addition of extrinsic dopants reduces the work function of ZnO, which leads to enhanced field-effect passivation by reducing the hole concentration at the c-Si surface.

The doped ZnO films described in this work are highly transparent, conductive, suitable as anti-reflection coating, and moreover provide high levels of surface passivation. Due to these properties, the ZnO films provide new opportunities for c-Si solar cells. For instance, the ZnO films could potentially serve as an alternative to SiN_x as a passivating anti-reflection coating at the front surface of solar cells. In this way, it would loosen the lateral conduction requirements of the emitter or omit the use of firing-through metallization. Moreover, the passivating ZnO films are of specific interest as a highly transparent passivating electron contact. For this application to be successful, a sufficiently low contact resistivity of passivating ZnO with c-Si will be a prerequisite.[47,48] Finally, it is expected that the approach and insights presented in this work will be more generally applicable and can aid the development of other (emerging) surface passivation and passivating contact materials.

SUPPLEMENTARY MATERIAL

See the supplementary material for a more in-depth study on the influence of the ZnO film thickness on the passivation quality. Moreover, it provides the *n* and *k* values of the ZnO film of Table I that are used for OPAL2 simulations.

ACKNOWLEDGMENTS

The authors gratefully acknowledge Dr. G. Yang, Dr. M. A. Verheijen, Dr. B. Barcones Campo, Dr. R. H. J. Vervuurt,

M. Dielen, and R. W. H. S. Scheerder from the Eindhoven University of Technology for experimental support. Dr. L. E. Black is acknowledged for fruitful discussions and feedback. Dr. J. van Berkum from Philips Innovation Services is acknowledged for SIMS analysis. We thank Air Liquide for providing us with deuterated TMA. This work was funded by the Dutch Ministry of Economic Affairs, through the Topconsortia for Knowledge and Innovation (TKI) programs AAA and Compass. The work of J. Melskens was supported by the Netherlands Organisation for Scientific Research under the Dutch TTW-VENI Grant No. 15896. The Solliance Solar Research consortium and the Dutch province of Noord-Brabant are acknowledged for funding the TEM facility.

REFERENCES

[1]W. Shockley and W. T. J. Read, "Statistics of the recombinations of holes and electrons," Phys. Rev. **87**(5), 835–842 (1952).
[2]R. N. Hall, "Electron-hole recombination in germanium," Phys. Rev. **87**, 387 (1952).
[3]L. E. Black, B. W. H. van de Loo, B. Macco, J. Melskens, W. J. H. Berghuis, and W. M. M. Kessels, "Explorative studies of novel silicon surface passivation materials: Considerations and lessons learned," Sol. Energy Mater. Sol. Cells **188**, 182–189 (2018).
[4]G. Krugel, A. Sharma, W. Wolke *et al.*, "Study of hydrogenated AlN as an anti-reflective coating and for the effective surface passivation of silicon," Phys. Status Solidi—Rapid Res. Lett. **7**(7), 457–460 (2013).
[5]B. Liao, B. Hoex, A. G. Aberle *et al.*, "Excellent c-Si surface passivation by low-temperature atomic layer deposited titanium oxide," Appl. Phys. Lett. **104**(25), 253903 (2014).
[6]T. G. Allen and A. Cuevas, "Electronic passivation of silicon surfaces by thin films of atomic layer deposited gallium oxide," Appl. Phys. Lett. **105**(2014), 31601 (2014).
[7]Y. Wan, J. Bullock, and A. Cuevas, "Tantalum oxide/silicon nitride: A negatively charged surface passivation stack for silicon solar cells," Appl. Phys. Lett. **106**(20), 201601 (2015).
[8]J. Cui, Y. Wan, Y. Cui *et al.*, "Highly effective electronic passivation of silicon surfaces by atomic layer deposited hafnium oxide," Appl. Phys. Lett. **110**(2), 021602 (2017).
[9]L. E. Black and W. M. M. (Erwin) Kessels, "PO_x/Al_2O_3 stacks: Highly effective surface passivation of crystalline silicon with a large positive fixed charge," Appl. Phys. Lett., **112**(20), 201603 (2018).
[10]B. Macco, L. E. Black, J. Melskens *et al.*, "Atomic-layer deposited Nb_2O_5 as transparent passivating electron contact for c-Si solar cells," Sol. Energy Mater. Sol. Cells **184**(April), 98–104 (2018).
[11]Y. Wan, J. Bullock, M. Hettick *et al.*, "Zirconium oxide surface passivation of crystalline silicon," Appl. Phys. Lett. **112**(20), 201604 (2018).
[12]Y. Wu, P. M. Hermkens, B. W. H. van de Loo *et al.*, "Electrical transport and Al doping efficiency in nanoscale ZnO films prepared by atomic layer deposition," J. Appl. Phys. **114**(2), 24308 (2013).
[13]D. Garcia-Alonso, S. E. Potts, C. A. A. van Helvoirt *et al.*, "Atomic layer deposition of B-doped ZnO using triisopropyl borate as the boron precursor and comparison with Al-doped ZnO," J. Mater. Chem. C **3**(13), 3095–3107 (2015).
[14]B. Macco, D. Deligiannis, S. Smit *et al.*, "Influence of transparent conductive oxides on passivation of a-Si:H/c-Si heterojunctions as studied by atomic layer deposited Al-doped ZnO," Semicond. Sci. Technol. **29**(12), 122001 (2014).
[15]N. Nandakumar, B. Hoex, B. Dielissen *et al.*, "Conductive gallium-doped ZnO films deposited by ultrafast spatial atomic layer deposition for photovoltaic application," in *25th Asia Photovoltaic Solar Energy Conference and Exhibition* (2015).
[16]B. Macco, H. C. M. Knoops, M. A. Verheijen *et al.*, "Atomic layer deposition of high-mobility hydrogen-doped zinc oxide," Sol. Energy Mater. Sol. Cells **173**, 111–119 (2017).
[17]R. Peibst, Y. Larionova, S. Reiter *et al.*, "Building blocks for industrial, screen-printed double-side contacted POLO cells with highly transparent ZnO:Al layers," IEEE J. Photovoltaics **8**(3), 719–725 (2018).
[18]K. Kajiyama and Y. Furukawa, "Electrical and optical properties of SnO_2-Si heterojunctions," Jpn. J. Appl. Phys. **6**, 905–606 (1967).
[19]P. Stradins, S. Essig, W. Nemeth *et al.*, "Passivated tunneling contacts to n-type wafer silicon and their implementation into high performance solar cells preprint," in *6th World Conference on Photovoltaic Energy Conversion*, Kyoto, Japan, 23–27 November 2014 (NREL, 2014).
[20]F. Wang, S. Zhao, B. Liu *et al.*, "Silicon solar cells with bifacial metal oxides carrier selective layers," Nano Energy **39**, 437–443 (2017).
[21]J. Ding, Y. Zhou, G. Dong *et al.*, "Solution-processed ZnO as the efficient passivation and electron selective layer of silicon solar cells," Prog. Photovolt. Res. Appl. **26**, 974–980 (2018).
[22]S. Smit, D. Garcia-Alonso, S. Bordihn *et al.*, "Metal-oxide-based hole-selective tunneling contacts for crystalline silicon solar cells," Sol. Energy Mater. Sol. Cells **120**, 376–382 (2014).
[23]J. Panigrahi, S. R. Vandana *et al.* Crystalline silicon surface passivation by thermal ALD deposited Al doped ZnO thin films. AIP Adv. **7**(3), 35219 (2017).
[24]C. Battaglia, S. M. de Nicolás, S. De Wolf *et al.*, " Silicon heterojunction solar cell with passivated hole selective MoOx contact," Appl. Phys. Lett. **104**(11), 113902 (2014).
[25]L. G. Gerling, S. Mahato, A. Morales-Vilches *et al.*, "Transition metal oxides as hole-selective contacts in silicon heterojunctions solar cells," Sol. Energy Mater. Sol. Cells **145**, 109–115 (2016).
[26]A. Moldovan, F. Feldmann, M. Zimmer *et al.*, "Tunnel oxide passivated carrier-selective contacts based on ultra-thin SiO_2 layers," Sol. Energy Mater. Sol. Cells **142**, 123–127 (2015).
[27]S. Lindekugel, H. Lautenschlager, T. Ruof, and S. Reber, "Plasma hydrogen passivation for crystalline silicon thin-films," in *23rd EU-PVSEC*, Valencia, Spain (2008), pp. 2232–2235.
[28]M. K. Stodolny, M. Lenes, Y. Wu *et al.*, "n-Type polysilicon passivating contact for industrial bifacial n-type solar cells," Sol. Energy Mater. Sol. Cells **158**, 24–28 (2016).
[29]F. Feldmann, M. Simon, M. Bivour *et al.*, "Carrier-selective contacts for Si solar cells," Appl. Phys. Lett. **104**(18), 181105 (2014).
[30]B. Nemeth, D. L. Young, M. R. Page *et al.*, "Polycrystalline silicon passivated tunneling contacts for high efficiency silicon solar cells," J. Mater. Res. **31**(6), 671–681 (2016).
[31]M. Schnabel, B. W. H. van de Loo, W. Nemeth *et al.*, "Hydrogen passivation of poly-Si/SiOx contacts for Si solar cells using Al_2O_3 studied with deuterium," Appl. Phys. Lett. **112**(20), 203901 (2018).
[32]W. Kern, "Cleaning solutions based on hydrogen peroxide for use in silicon semiconductor technology," RCA Rev. **31**, 187–206 (1970).
[33]H. C. M. Knoops, B. W. H. van de Loo, S. Smit *et al.*, "Optical modeling of plasma-deposited ZnO films: Electron scattering at different length scales," J. Vac. Sci. Technol. A **33**(2), 21509 (2015).
[34]A. Richter, S. W. Glunz, F. Werner *et al.*, "Improved quantitative description of Auger recombination in crystalline silicon," Phys. Rev. B **86**(16), 165202 (2012).
[35]K. R. McIntosh and S. C. Baker-Finch, "OPAL 2: Rapid optical simulation of silicon solar cells," in *2012 38th IEEE Photovoltaic Specialist Conference* (IEEE, 2012), pp. 000265–000271.
[36]X. Yang, Q. Bi, H. Ali *et al.*, "High-performance TiO_2-based electron-selective contacts for crystalline silicon solar cells," Adv. Mater. **28**(28), 5891–5897 (2016).
[37]D. L. Young, W. Nemeth, S. Grover *et al.*, "Carrier-selective, passivated contacts for high efficiency silicon solar cells based on transparent conducting oxides," in *2014 IEEE 40th Photovoltaic Specialist Conference* (IEEE, 2014), Vol. **0**, pp. 1–5.
[38]X. Yang, P. Zheng, Q. Bi, and K. Weber, "Silicon heterojunction solar cells with electron selective TiOx contact," Sol. Energy Mater. Sol. Cells **150**, 32–38 (2016).

[39]W. Beyer, U. Breuer, F. Hamelmann *et al.*, "Hydrogen diffusion in zinc oxide thin films," MRS Proc. **1165**, 1165-M05-24 (2009).
[40]G. Dingemans, F. Einsele, W. Beyer *et al.*, "Influence of annealing and Al_2O_3 properties on the hydrogen-induced passivation of the Si/SiO_2 interface," J. Appl. Phys. **111**(9), 93713 (2012).
[41]K. G. Sun, Y. V. Li, D. B. Saint John, and T. N. Jackson, "pH-controlled selective etching of Al_2O_3 over ZnO," ACS Appl. Mater. Interfaces, **6**, 7028 –7031 (2014).
[42]G. Dingemans, W. Beyer, M. C. M. van de Sanden, and W. M. M. Kessels, "Hydrogen induced passivation of Si interfaces by Al_2O_3 films and SiO_2/Al_2O_3 stacks," Appl. Phys. Lett. **97**(15), 152106 (2010).
[43]G. Dingemans, C. A. A. van Helvoirt, D. Pierreux *et al.*, "Plasma-assisted ALD for the conformal deposition of SiO_2: Process, material and electronic properties," J. Electrochem. Soc. **159**(3), H277–H285 (2012).
[44]E. Burstein, "Anomalous optical absorption limit in InSb," Phys. Rev. **93**(3), 632 (1954).
[45]T. S. Moss, "The interpretation of the properties of indium antimonide," Proc. Phys. Soc. B **67**(10), 775–782 (1954).
[46]K. Ellmer and R. Mientus, "Carrier transport in polycrystalline ITO and ZnO:Al II: The influence of grain barriers and boundaries," Thin Solid Films **516**(17), 5829–5835 (2008).
[47]J. Melskens, B. W. H. van de Loo, B. Macco *et al.*, " Passivating contacts for crystalline silicon solar cells: From concepts and materials to prospects," IEEE J. Photovoltaics **8**(2), 373–388 (2018).
[48]B. Macco, B. W. H. van de Loo, and W. M. M. Kessels, "Atomic layer deposition for high efficiency crystalline silicon solar cells," in *Atomic Layer Deposition in Energy Conversion Applications*, edited by J. Bachmann (Wiley, 2017).